Four-body continuum-distorted-wave model for charge exchange between hydrogenlike projectiles and atoms

Ivan Mančev
Department of Physics, Faculty of Sciences and Mathematics, P.O. Box 224, 18000 Niš, Serbia
(Received 5 February 2007; published 24 May 2007)

The four-body continuum-distorted-wave model is formulated and used to investigate single electron capture in fast collisions of hydrogenlike projectiles with one- and multi-electron targets. The presented method of an analytical calculation of scattering integrals yields the total cross sections in terms of four-dimensional numerical quadratures. As an illustration, total cross sections are computed for electron capture processes in He^+-H, He^+-He, and Li^{2+}-He collisions at intermediate and high impact energies. The contribution from the interelectron interaction during the collision is evaluated. The prior and post total cross sections are found to be in good agreement with the available experimental data.

DOI: 10.1103/PhysRevA.75.052716 PACS number(s): 34.70.+e, 82.30.Fi

I. INTRODUCTION

Single electron capture from one- and multi-electron atoms colliding with *hydrogenlike* projectiles has received much attention from experimentalists for decades (see, for example, Atan *et al.* [1], Forest *et al.* [2], DuBois [3], Hvelplund and Andersen [4], de Castro Faria *et al.* [5], Woitke *et al.* [6], Olson [7], Shah *et al.* [8], Murphy *et al.* [9], Itoh *et al.* [10], and Pivovar *et al.* [11]). However, theoretical investigations of such processes have been less extensive, mainly due to the difficulties which arise in an adequate representation of collision systems that are more complex than a three-body problem. The calculations are usually simplified by approximating a many-electron collision system by a model with only one active electron. In other words, among all the electrons in the target, only the captured electron is viewed as being active. The net result of such a simplified model is a reduction of the many-particle problem to a three-body problem.

Charge transfer cross sections in collisions of partially stripped projectiles with atomic hydrogen have been studied via different three-body methods such as: the boundary corrected continuum intermediate state approximation (BCIS) [12], the Coulomb-Born (CB) model [13], and the Oppenheimer-Brinkman-Kramers (OBK) approximation [14].

The three-body continuum distorted wave (CDW-3B) approach has been applied by Belkić [15] to study charge-exchange collisions between hydrogenlike projectiles (Li^{2+}, B^{4+}, C^{5+}, N^{6+}, and O^{7+}) and a hydrogen atom. The corresponding results were obtained by considering the incident particles as the corresponding screened nuclei.

Electron capture and ionization in terms of the classical trajectory Monte Carlo (CTMC) were investigated in Refs. [12,16–18] for collision of different partially stripped projectile ions with a hydrogen atom as a target. The CTMC method treats the particles in collision as classical point particles which interact through the Coulomb law, while their motion is governed by the Newton dynamics. In Refs. [12,18], the interaction of the captured (active) electron with the partially stripped projectile ion has been approximated by a non-Coulombic model potential. Although such three-body models show a satisfactory agreement with experimental data, these methods completely neglect dynamic (i.e., collisional) correlations. A substantially different approach to the problem of high-energy electron capture from one- and multi-electron atoms by hydrogenlike projectiles has recently been undertaken by Mančev [19,20], who introduced the four-body corrected first Born (CB1-4B) approximation for these processes.

In the present work the four-body continuum distorted wave (CDW-4B) model is formulated for single electron transfer in collisions (i) between two hydrogenlike atoms including all the Coulomb interactions, and (ii) from multi-electron atoms by hydrogenlike projectiles. In both processes (i) and (ii), the captured electron from the target and the projectile electron are treated as active. Simultaneously, the remaining noncaptured electrons from the target are considered as passive. The validity of the proposed CDW-4B model is assessed in comparison with the available experimental data for total cross sections. Thus far, single charge exchange in fast collisions of *completely stripped projectiles* with heliumlike targets has been studied by means of the CDW-4B approximation [21–23]. Different four-body distorted wave methods for various inelastic high-energy ion-atom collisions (single and double capture, ionization, transfer-excitation, transfer-ionization, etc.) have recently been analyzed in Refs. [24–27].

Understanding the role of the electron-electron correlations is of great topical interest. Four-body treatments allow one to study the effects of the electron-electron correlations in single capture. Along these lines, the suggested CDW-4B approximation is utilized in the present work to acquire the important information about the relative significance of the role of the dynamic interelectron interaction in He^+-H, He^+-He, and Li^{2+}-He collisions. The role of interelectron correlation effects in these processes has not been previously established. Atomic units will be used throughout unless otherwise stated.

II. THEORY

We examine single electron capture in two types of collisions, such as a collision between hydrogenlike projectiles

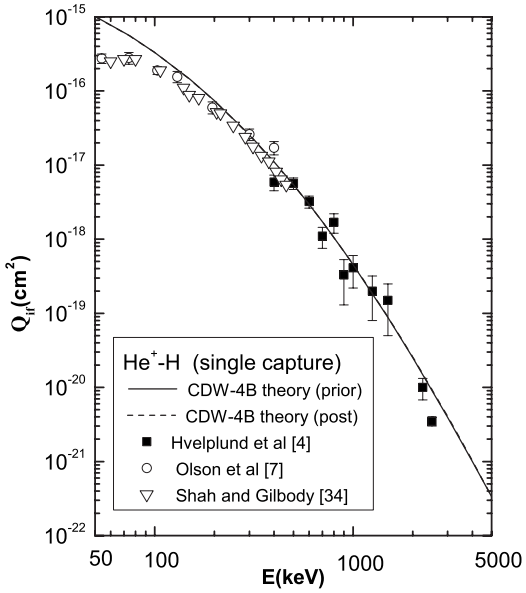

FIG. 1. Total cross sections (in cm^2) as a function of the laboratory incident energy for reaction $^4He^+ + H \rightarrow {}^4He + H^+$. The full and dashed curves represent the prior and post total cross sections, respectively. Both theoretical curves are obtained with the complete perturbation potentials. The final ground state of atom $He(1s^2)$ is described by means of the Silverman *et al.*'s [33] orbital. Experimental data: ■, Hvelplund and Andersen [4]; ○, Olson *et al.* [7]; and ▽, Shah and Gilbody [34].

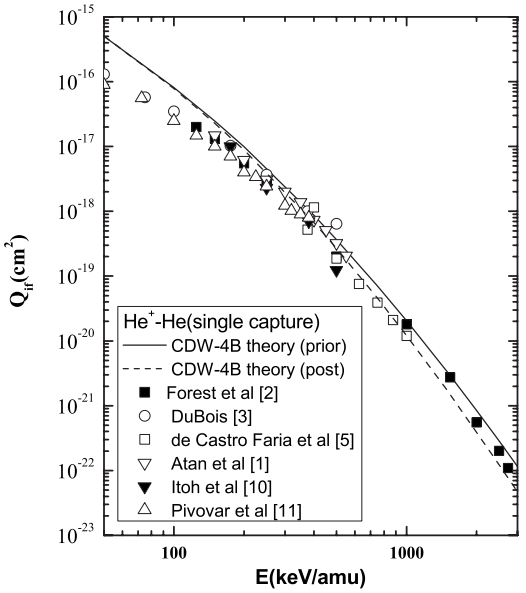

FIG. 2. Total cross sections (in cm^2) as a function of the laboratory incident energy for reaction $^4He^+ + {}^4He \rightarrow {}^4He + {}^4He^+$. The full and the dashed curves represent the prior and post total cross sections, respectively. Both theoretical curves are obtained with the complete perturbation potentials. The final ground state of atom $He(1s^2)$ is described by means of the Silverman *et al.*'s [33] orbital, whereas the RHF wave function is employed for the target atom. Experimental data: ■, Forest *et al.* [2]; ○, DuBois [3]; □, de Castro Faria *et al.* [5]; ▽, Atan *et al.* [1]; ▼, Itoh *et al.* [10]; and △, Pivovar *et al.* [11].

and hydrogenlike targets as well as those involving multielectron targets:

$$(Z_P,e_1) + (Z_T,e_2) \rightarrow (Z_P,e_1,e_2) + Z_T, \tag{1}$$

$$(Z_P,e_1) + (Z_T,e_2;\{e_3,e_4,\ldots,e_{N+2}\}) \rightarrow (Z_P,e_1,e_2) + (Z_T;\{e_3,e_4,\ldots,e_{N+2}\}), \tag{2}$$

where $\{e_3,e_4,\ldots,e_{N+2}\}$ denotes the N noncaptured electrons. Here, the small brackets symbolize the bound states. Let $\vec{s}_1$ and $\vec{s}_2$ ($\vec{x}_1$ and $\vec{x}_2$) be position vectors of the first and the second electrons (e_1 and e_2) relative to the nuclear charge of the projectile Z_P (the target Z_T). Further, let $\vec{R}$ be the position vector of Z_T with respect to Z_P. The vector of the distance between the two active electrons (e_1 and e_2) is labeled as $\vec{r}_{12}=\vec{x}_1-\vec{x}_2=\vec{s}_1-\vec{s}_2$. In the entrance channel, it is convenient to introduce $\vec{r}_i$ as the position vector between the center of mass of (Z_P,e_1) and the target system. Symmetrically, in the exit channel, let $\vec{r}_f$ be the position vector of the center of mass of (Z_P,e_1,e_2) relative to Z_T.

In the case of a multielectron target, we shall introduce the following assumptions. All the N noncaptured electrons are considered as passive, such that their interactions with both active electrons e_1 and e_2 do not contribute to the capture process. We also suppose that passive electrons occupy the same orbitals before and after the collisions. The final state of the target rest is ignored in such a single-particle approximation. In this model, passive electrons do not participate individually in the transfer of the active electron, and we can use an effective local target potential V_T. In the present work, we shall employ the Roothan-Hartree-Fock (RHF) model. According to this model, the effective target potential V_T is used as a pure Coulomb target potential $V_T(x_2)=-Z_T^{ef}/x_2$, where Z_T^{ef} is an effective nuclear charge. The value of the Z_T^{ef} is determined as suggested by Belkić *et al.* [29] via $Z_T^{ef}=n_i(-2E_T^{RHF})^{1/2}$, where E_T^{RHF} is the RHF orbital energy obtained variationally by Clementi and Roetti [30], and n_i is the principal quantum number of the target electron to be captured. The initial bound state of the target active electron (e_2) is described by the RHF wave function which can be expressed as a linear combination of the normalized Slater-type orbitals:

$$\varphi_T^{RHF}(\vec{x}_2) = \sum_{k=1}^{N_i} C_k \chi_{n_k l_i m_i}^{(\alpha_k)}(\vec{x}_2), \tag{3}$$

$$\chi_{n_k l_i m_i}(\vec{x}_2) = \sqrt{\frac{(2\alpha_k)^{1+2n_k}}{(2n_k)!}} r^{n_k-1} e^{-\alpha_k r} Y_{l_i,m_i}(\hat{\vec{x}}_2), \tag{4}$$

where C_k and α_k are parameters obtained by Clementi and Roetti [30], whereas n_k is the orbital number. In this way, the multielectron process (2) is reduced to a four-body problem:

$$(Z_P,e_1) + (Z_T^{ef},e_2) \rightarrow (Z_P,e_1,e_2) + Z_T^{ef}. \tag{5}$$

The prior and post forms of the transition amplitudes in the CDW-4B approximation are given by the matrix elements:

$$T_{if}^{-} = \langle \chi_f^{-} | U_i | \chi_i^{+} \rangle, \quad T_{if}^{+} = \langle \chi_f^{-} | U_f^{\dagger} | \chi_i^{+} \rangle. \tag{6}$$

The choice of the perturbation potentials U_i and U_f as

$$U_i = Z_T^{ef}\left(\frac{1}{R} - \frac{1}{x_1}\right) - \frac{1}{s_2} + \frac{1}{r_{12}} - \vec{\nabla}_{x_2} \ln \varphi_T(\vec{x}_2) \cdot \vec{\nabla}_{s_2}, \tag{7}$$

$$U_f = Z_T^{ef}\left(\frac{1}{R} - \frac{1}{x_1}\right) - \vec{\nabla}_{s_2} \ln \varphi_f(\vec{s}_1, \vec{s}_2) \cdot \vec{\nabla}_{x_2}, \tag{8}$$

together with eikonal approximation $\vec{R} \simeq -\vec{r}_f$, $\vec{R} \simeq \vec{r}_i$, provides the distorted waves $\chi_{i,f}^{\pm}$ as follows:

$$\chi_i^{+} = N^{+}(\nu_P)\mathcal{N}^{+}(\nu) e^{i\vec{k}_i \cdot \vec{r}_i} \varphi_P(\vec{s}_1)\varphi_T(\vec{x}_2) {}_1F_1(i\nu_P, 1, i\upsilon s_2 + i\vec{\upsilon} \cdot \vec{s}_2) {}_1F_1(-i\nu, 1, ik_i r_i - i\vec{k}_i \cdot \vec{r}_i), \tag{9}$$

$$\chi_f^{-} = N^{-}(\nu_T)\mathcal{N}^{-}(\nu) e^{-i\vec{k}_f \cdot \vec{r}_f} \varphi_f(\vec{s}_1, \vec{s}_2) {}_1F_1(-i\nu_T, 1, -i\upsilon x_2 - i\vec{\upsilon} \cdot \vec{x}_2) {}_1F_1(i\nu, 1, -ik_f r_f + i\vec{k}_f \cdot \vec{r}_f), \tag{10}$$

where $\nu_P = (Z_P - 1)/\upsilon$, $\nu_T = Z_T^{ef}/\upsilon$, $\nu = Z_T^{ef}(Z_P - 1)/\upsilon$, and $N^{-}(\nu_T) = \Gamma(1 + i\nu_T)e^{\pi\nu_T/2}$, $N^{+}(\nu_P) = \Gamma(1 - i\nu_P)e^{\pi\nu_P/2}$, $\mathcal{N}^{\pm}(\nu) = \Gamma(1 \pm i\nu)e^{-\pi\nu/2}$. The incident velocity vector $\vec{\upsilon}$ is chosen as $\vec{\upsilon} = (0, 0, \upsilon)$. The symbol ${}_1F_1(a, b, z)$ stands for the regular confluent hypergeometric function. The hydrogenlike wave function of the (Z_P, e_1) system is denoted as $\varphi_P(\vec{s}_1)$, and the corresponding binding energy is E_P, whereas $\varphi_f(\vec{s}_1, \vec{s}_2)$ is the bound state wave function of the heliumlike atomic system (Z_P, e_1, e_2) with the binding energy E_f. The vectors $\vec{k}_i$ and $\vec{k}_f$ are the initial and final momenta, respectively. It is readily verified that the distorted waves $\chi_{i,f}^{\pm}$ satisfy the proper boundary conditions. It should be noted that variables $\{\vec{x}_1, \vec{x}_2, \vec{R}\}$ and $\{\vec{s}_1, \vec{x}_2, \vec{R}\}$ are treated as independent, despite the fact that $\vec{R} = \vec{x}_1 - \vec{s}_1 = \vec{x}_2 - \vec{s}_2$, and they can be called the generalized nonorthogonal coordinates [28]. The appearance of the $\nabla \cdot \nabla$ operator as a perturbation operator in distorted wave methods has extensively been discussed by Crothers and Dubé [28].

The explicit expressions for the matrix elements of the transition amplitudes $T_{if}^{\pm}$ take the following forms:

$$T_{if}^{+}(\vec{\eta}) = N^{-*}(\nu_T)N^{+}(\nu_P) \int\int\int d\vec{x}_1 d\vec{x}_2 d\vec{R} e^{i\vec{\alpha}\cdot\vec{s}_2 + i\vec{\beta}\cdot\vec{x}_2} \varphi_P(\vec{s}_1)\varphi_T(\vec{x}_2) F(i\nu_P, 1, i\upsilon s_2 + i\vec{\upsilon}\cdot\vec{s}_2) \left\{ Z_T^{ef}\left(\frac{1}{R} - \frac{1}{x_1}\right)\varphi_f^{*}(\vec{s}_1, \vec{s}_2) F(i\nu_T, 1, i\upsilon x_2 + i\vec{\upsilon}\cdot\vec{x}_2) - \vec{\nabla}_{s_2}\varphi_f^{*}(\vec{s}_1, \vec{s}_2)\cdot\vec{\nabla}_{x_2} F(i\nu_T, 1, i\upsilon x_2 + i\vec{\upsilon}\cdot\vec{x}_2) \right\}, \tag{11}$$

$$T_{if}^{-}(\vec{\eta}) = N^{-*}(\nu_T)N^{+}(\nu_P) \int\int\int d\vec{x}_1 d\vec{x}_2 d\vec{R} e^{i\vec{\alpha}\cdot\vec{s}_2 + i\vec{\beta}\cdot\vec{x}_2} \varphi_f^{*}(\vec{s}_1, \vec{s}_2) F(i\nu_T, 1, i\upsilon x_2 + i\vec{\upsilon}\cdot\vec{x}_2) \left\{ \left[Z_T^{ef}\left(\frac{1}{R} - \frac{1}{x_1}\right) + \frac{1}{r_{12}} - \frac{1}{s_2} \right] \varphi_P(\vec{s}_1)\varphi_T(\vec{x}_2) F(i\nu_P, 1, i\upsilon s_2 + i\vec{\upsilon}\cdot\vec{s}_2) - \varphi_P(\vec{s}_1)\vec{\nabla}_{x_2}\varphi_T(\vec{x}_2)\cdot\vec{\nabla}_{s_2} F(i\nu_P, 1, i\upsilon s_2 + i\vec{\upsilon}\cdot\vec{s}_2) \right\}. \tag{12}$$

The following product is simplified as [29]: $\mathcal{N}^{-*}(\nu)\mathcal{N}^{+}(\nu) {}_1F_1(-i\nu, 1, ik_f r_f - i\vec{k}_f\cdot\vec{r}_f) {}_1F_1(-i\nu, 1, ik_i r_i - i\vec{k}_i\cdot\vec{r}_i) \simeq (\rho\upsilon)^{Z_T^{ef}(Z_P-1)/\upsilon}$, where $\vec{\rho}$ is a component of the vector of the internuclear distance perpendicular to the Z-axis. The multiplying factor $(\rho\upsilon)^{Z_T^{ef}(Z_P-1)/\upsilon}$ is ignored in Eqs. (11) and (12), since it does not contribute to the total cross section. In addition to this simplification, we shall also use the eikonal hypothesis, since the small-angle limit applies to heavy particles so that:

$$\vec{k}_i\cdot\vec{r}_i + \vec{k}_f\cdot\vec{r}_f = \vec{\alpha}\cdot\vec{s}_2 + \vec{\beta}\cdot\vec{x}_2 = -\vec{\upsilon}\cdot\vec{s}_2 + \vec{\beta}\cdot\vec{R},$$

where the momentum transfers $\vec{\alpha}$ and $\vec{\beta}$ are defined by

$$\vec{\beta} = -\vec{\eta} - \beta_z\hat{\vec{\upsilon}}, \quad \vec{\alpha} = \vec{\eta} - \alpha_z\hat{\vec{\upsilon}}, \quad \vec{\alpha} + \vec{\beta} = -\vec{\upsilon},$$

$$\alpha_z = \upsilon/2 - \Delta E/\upsilon, \quad \beta_z = \upsilon/2 + \Delta E/\upsilon, \quad \Delta E = E_P + E_T^{RHF} - E_f.$$

The transverse component of the change in the relative linear momentum of a heavy particle is denoted by $\vec{\eta} = (\eta\cos\phi_\eta, \eta\sin\phi_\eta, 0)$. When the above expressions are used for one-electron targets, the pair $\{Z_T^{ef}, E_T^{RHF}\}$ should be replaced by $\{Z_T, E_T\}$, where $E_T = -Z_T^2/(2n_i^2)$.

In the present paper, as an illustration of collisions of the type (2), a helium atom is used for the target. The RHF wave function, given by Clementi and Roetti [30] for He(^1S) can be written in the form:

$$\varphi_T^{RHF}(\vec{r}) = \frac{1}{\sqrt{\pi}}\sum_{i=1}^{5} C_i e^{-\zeta_i r}, \tag{13}$$

with $C_1 = 1.296\,27$; $C_2 = 0.818\,831$; $C_3 = 0.376\,271$; $C_4 = -0.165\,751$; $C_5 = 0.051\,483$; $\zeta_1 = 1.417\,14$; $\zeta_2 = 2.376\,82$; $\zeta_3 = 4.396\,28$; $\zeta_4 = 6.526\,99$; $\zeta_5 = 7.942\,52$, $E_T^{RHF} = -0.917\,95$, and $Z_T^{ef} = 1.354\,954$. We have assumed the general factorized form for the bound state of the newly formed heliumlike atom (or ion) $(Z_P, e_1, e_2)_{1s^2}$:

$$\varphi_f(\vec{s}_1, \vec{s}_2) = \sum_{k,l} \varphi_{\alpha k}(\vec{s}_1)\varphi_{\alpha l}(\vec{s}_2), \tag{14}$$

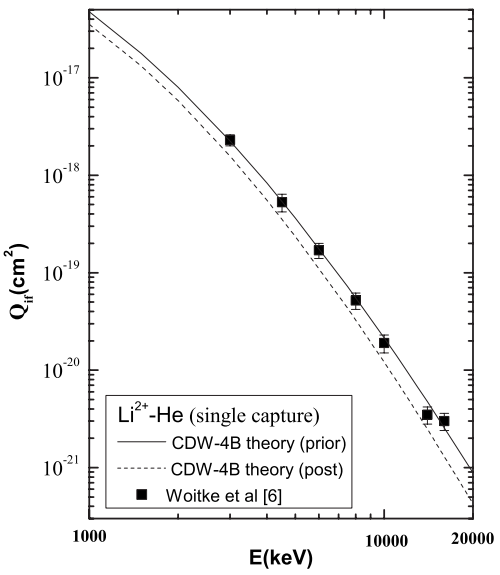

FIG. 3. Total cross sections (in cm^2) as a function of the laboratory incident energy for reaction $^7Li^{2+}+{}^4He \rightarrow {}^7Li^{+}+{}^4He^{+}$. The full and dashed curves represent the prior and post total cross sections, respectively. Both theoretical curves are obtained with the complete perturbation potentials. The final ground state of the $Li^{+}(1s^2)$ ion is described by means of the Silverman *et al.*'s orbital [33], whereas the RHF wave function is employed for the target atom. Experimental data: ■, Woitke *et al.* [6].

where $\varphi_{\alpha j}(\vec{r})=N_{\alpha_j}\exp(-\alpha_j r)$, $N_{\alpha_j}=a_j\sqrt{N}$ $(j=k,l)$, and N is the normalization constant. The values of the summation indices k and l, as well as the variationally determined parameters α_j and a_j, depend upon a concrete choice of the wave function.

Employing the well-known relationship:

$$\frac{1}{\omega}=\frac{1}{2\pi^2}\int\frac{d\vec{p}}{p^2}e^{-i\vec{p}\cdot\vec{\omega}} \tag{15}$$

for $\omega=\{\vec{r}_{12},\vec{R},\vec{x}_1\}$, and applying the Nordsieck [31] complex integration, the expressions for the transition amplitudes become

$$T_{if}^{-}=\mathcal{M}\sum_{i=1}^{5}C_i\sum_{k,l}N_{\alpha_k}N_{\alpha_l}\left[-\mathcal{U}_{\nabla}^{-}-\mathcal{U}_{s_2}+\frac{Z_T^{ef}}{2\pi^2}\int\frac{d\vec{p}}{p^2}(\mathcal{U}_{Rx_1}+\mathcal{U}_{12})\right], \tag{16}$$

$$T_{if}^{-}=\mathcal{M}\sum_{i=1}^{5}C_i\sum_{k,l}N_{\alpha_k}N_{\alpha_l}\left[-\mathcal{U}_{\nabla}^{-}-\mathcal{U}_{s_2}+\frac{Z_T^{ef}}{2\pi^2}\int_0^{\infty}dp\int_0^{\pi}\cos\theta_p d\theta_p\int_0^{2\pi}d\phi_p(\mathcal{U}_{Rx_1}+\mathcal{U}_{12})\right], \tag{17}$$

$$T_{if}^{+}=\mathcal{M}\sum_{i=1}^{5}C_i\sum_{k,l}N_{\alpha_k}N_{\alpha_l}\left[-\mathcal{U}_{\nabla}^{+}+\frac{Z_T^{ef}}{2\pi^2}\int\frac{d\vec{p}}{p^2}\mathcal{U}_{Rx_1}\right], \tag{18}$$

where $\mathcal{M}=2^9\pi^2Z_P^{3/2}N^{-*}(\nu_T)N^{+}(\nu_P)$. All the other quantities appearing in the above expressions are defined as follows:

$$\mathcal{U}_{\nabla}^{-}=\frac{i\nu_P v\zeta_i}{(Z_P+\alpha_l)^3}\frac{T_0^{i\nu_P+1}R_0^{i\nu_T}[(1-i\nu_T)\vec{\beta}-i\nu_T\vec{\alpha}R_0]\cdot(\alpha_k\hat{\vec{v}}+i\vec{\alpha})}{(\alpha^2+\alpha_k^2)^2(\beta^2+\zeta^2)^2}, \tag{19}$$

$$\mathcal{U}_{\nabla}^{+}=\frac{i\nu_T v\alpha_k}{(Z_P+\alpha_l)^3}\frac{T_0^{i\nu_P}R_0^{i\nu_T+1}[(1-i\nu_P)\vec{\alpha}-i\nu_P\vec{\beta}T_0]\cdot(\zeta_i\hat{\vec{v}}+i\vec{\beta})}{(\alpha^2+\alpha_k^2)^2(\beta^2+\zeta_i^2)^2}, \tag{20}$$

$$\mathcal{U}_{Rx_1}=\left\{\frac{1}{(Z_P+\alpha_l)^3}-\frac{(Z_P+\alpha_l)}{[p^2+(Z_P+\alpha_l)^2]^2}\right\}\frac{T_+^{i\nu_P}R_-^{i\nu_T}\mathcal{T}_{+,-}}{(|\vec{\alpha}+\vec{p}|^2+\alpha_k^2)^2(|\vec{\beta}-\vec{p}|^2+\zeta_i^2)^2}, \tag{21}$$

$$\mathcal{U}_{s_2}=\frac{T_0^{i\nu_P}R_0^{i\nu_T}[\zeta_i(1-i\nu_T)+i\nu_T(\zeta_i-iv)R_0]}{2(Z_P+\alpha_l)^2(\alpha^2+\alpha_k^2)(\beta^2+\zeta_i^2)^2}, \tag{22}$$

$$\mathcal{U}_{12}=\frac{(Z_P+\alpha_l)}{Z_T^{ef}}\frac{T_+^{i\nu_P}R_0^{i\nu_T}\mathcal{T}_{+,0}}{(\beta^2+\zeta_i^2)^2(|\vec{\alpha}+\vec{p}|^2+\alpha_k^2)^2[p^2+(Z_P+\alpha_l)]^2}, \tag{23}$$

$$\mathcal{T}_{+,0}=[\zeta_i(1-i\nu_T)+i\nu_T(\zeta_i-iv)R_0][\alpha_k(1-i\nu_P)+i\nu_P(\alpha_k-iv)T_+], \tag{24}$$

$$\mathcal{T}_{+,-}=[\zeta_i(1-i\nu_T)+i\nu_T(\zeta_i-iv)R_-][\alpha_k(1-i\nu_P)+i\nu_P(\alpha_k-iv)T_+], \tag{25}$$

$$T_0^{-1}=1+2\frac{\vec{\alpha}\cdot\vec{v}-i\alpha_k v}{\alpha^2+\alpha_k^2},\quad R_0^{-1}=1+2\frac{\vec{\beta}\cdot\vec{v}-i\zeta_i v}{\beta^2+\zeta_i^2}, \tag{26}$$

$$T_{\pm}^{-1}=1+2\frac{(\vec{\alpha}\pm\vec{p})\cdot\vec{v}-i\alpha_k v}{|\vec{\alpha}\pm\vec{p}|^2+\alpha_k^2},\quad R_{\pm}^{-1}=1+2\frac{(\vec{\beta}\pm\vec{p})\cdot\vec{v}-i\zeta_i v}{|\vec{\beta}\pm\vec{p}|^2+\zeta_i^2}. \tag{27}$$

Hence this method of calculation provides the basic matrix elements $T_{if}^{\pm}$ in the form of a three-dimensional integral over $\vec{p}=(p\sin\theta_p\cos\phi_p, p\sin\theta_p\sin\phi_p, p\cos\theta_p)$. The prior Q_{if}^{-} and post Q_{if}^{+} total cross sections in the CDW-4B approximation are given by

$$Q_{if}^{\pm}(\pi a_0^2)=\frac{1}{2\pi^2 v^2}\int_0^{\infty}d\eta\eta|T_{if}^{\pm}|^2. \tag{28}$$

In order to apply the Gauss-Legendre numerical quadrature for the integration over p, θ_p, and η, it is convenient to introduce the change of variables according to $p=(1+x)/(1-x)$, $x\in[-1,+1]$, $\cos\theta_p=u$, $u\in[-1,+1]$, $\eta=\sqrt{(1+\xi)/(1-\xi)}$, and $\xi\in[-1,+1]$. The remaining integra-

TABLE I. Total cross sections (in cm^2) as a function of the impact energy E for electron capture $^4He^+ + H \rightarrow {}^4He + H^+$. The displayed theoretical results are obtained by means of the CDW-4B model using the one-parameter Hylleraas wave function (labeled as "Hyll.") and the two-parameter Silverman *et al.*'s orbital [33] (denoted by "Silv.") for the final helium bound state. The quantities $Q_{if}^{\pm}$ represent the cross sections in the post (+) and prior (−) forms, respectively, obtained with the complete perturbation potentials according to Eqs. (11) and (12), whereas $Q_1^{\pm}$ refer to the cross sections computed with the additional approximation: $1/R=1/x_1$; Q_2^+ represents the cross sections obtained without the term $(1/r_{12}-1/s_2)$ in Eq. (12). The number in the square brackets denotes the powers of 10.

E (keV)	$\varphi_f(\vec{s}_1,\vec{s}_2)$	Q_{if}^-	Q_{if}^+	Q_1^-	Q_1^+	Q_2^-
50	Hyll.	1.11[−15]	1.18[−15]	9.77[−16]	1.03[−15]	1.74[−15]
	Silv.	1.07[−15]	1.01[−15]	8.93[−16]	8.84[−16]	1.60[−15]
75	Hyll.	5.95[−16]	6.06[−16]	5.38[−16]	5.49[−16]	8.43[−16]
	Silv.	5.53[−16]	5.49[−16]	5.01[−16]	4.97[−16]	7.93[−16]
100	Hyll.	3.56[−16]	3.57[−16]	3.29[−16]	3.32[−16]	4.67[−16]
	Silv.	3.32[−16]	3.30[−16]	3.08[−16]	3.06[−16]	4.41[−16]
150	Hyll.	1.57[−16]	1.56[−16]	1.49[−16]	1.49[−16]	1.83[−16]
	Silv.	1.45[−16]	1.44[−16]	1.39[−16]	1.38[−16]	1.72[−16]
300	Hyll.	2.85[−17]	2.89[−17]	2.85[−17]	2.90[−17]	2.75[−17]
	Silv.	2.57[−17]	2.54[−17]	2.60[−17]	2.58[−17]	2.48[−17]
500	Hyll.	6.17[−18]	6.39[−18]	6.34[−18]	6.59[−18]	5.12[−18]
	Silv.	5.46[−18]	5.41[−18]	5.74[−18]	5.70[−18]	4.51[−18]
700	Hyll.	1.96[−18]	2.06[−18]	2.05[−18]	2.16[−18]	1.47[−18]
	Silv.	1.72[−18]	1.72[−18]	1.86[−18]	1.85[−18]	1.28[−18]
1000	Hyll.	5.12[−19]	5.46[−19]	5.47[−19]	5.81[−19]	3.45[−19]
	Silv.	4.54[−19]	4.59[−19]	5.01[−19]	5.06[−19]	2.99[−19]
1500	Hyll.	9.72[−20]	1.03[−19]	1.06[−19]	1.12[−19]	5.68[−20]
	Silv.	8.76[−20]	8.96[−20]	9.90[−20]	1.01[−19]	4.96[−20]
2000	Hyll.	2.75[−20]	2.89[−20]	3.04[−20]	3.17[−20]	1.44[−20]
	Silv.	2.52[−20]	2.60[−20]	2.90[−20]	2.98[−20]	1.27[−20]
3000	Hyll.	4.23[−21]	4.25[−21]	4.75[−21]	4.76[−21]	1.88[−21]
	Silv.	3.96[−21]	4.07[−21]	4.64[−21]	4.76[−21]	1.68[−21]
4000	Hyll.	1.06[−21]	1.02[−21]	1.20[−21]	1.15[−21]	4.17[−22]
	Silv.	1.00[−21]	1.02[−21]	1.19[−21]	1.21[−21]	3.77[−22]
5000	Hyll.	3.50[−22]	3.24[−22]	3.98[−22]	3.71[−22]	1.26[−22]
	Silv.	3.36[−22]	3.37[−22]	4.01[−22]	4.02[−22]	1.15[−22]

tion over ϕ_p is performed by means of the Gauss-Mehler or the Gauss-Legendre quadrature. The singularities at the point $x=1$ and $\xi=1$ disappear altogether after analytical scaling of the integrand.

III. THE RESULTS OF NUMERICAL COMPUTATIONS

Numerical computations of the total cross sections are presently carried out for the following charge exchange reactions:

$$He^+ + H \rightarrow He + H^+, \tag{29}$$

$$He^+ + He \rightarrow He + He^+, \tag{30}$$

$$Li^{2+} + He \rightarrow Li^+ + He^+. \tag{31}$$

The computations are performed describing the final helium ground state by means of the one parameter Hylleraas orbital [32],

$$\varphi_f(\vec{s}_1,\vec{s}_2) = \frac{\alpha^3}{\pi} e^{-\alpha(x_1+x_2)}, \quad \alpha = Z_P - 5/16, \tag{32}$$

and the configuration interaction wave function $(1s1s')$ of Ref. [33] with the radial static correlations,

$$\varphi_f(\vec{s}_1,\vec{s}_2) = \frac{N}{\pi}(e^{-\alpha_1 x_1-\alpha_2 x_2} + e^{-\alpha_2 x_1-\alpha_1 x_2}), \tag{33}$$

TABLE II. Same as in Table I except for reaction $^4He^+ + {}^4He \rightarrow {}^4He + {}^4He^+$.

E (keV/amu)	$\varphi_f(\vec{s}_1,\vec{s}_2)$	Q_{if}^-	Q_{if}^+	Q_1^-	Q_1^+	Q_2^-
50	Hyll.	5.50[−16]	5.80[−16]	5.20[−16]	5.30[−16]	5.23[−16]
	Silv.	5.01[−16]	5.07[−16]	4.78[−16]	4.65[−16]	4.78[−16]
100	Hyll.	9.08[−17]	9.23[−17]	9.23[−17]	9.06[−17]	7.29[−17]
	Silv.	8.15[−17]	7.83[−17]	8.44[−17]	7.80[−17]	6.50[−17]
150	Hyll.	2.76[−17]	2.71[−17]	2.93[−17]	2.77[−17]	1.98[−17]
	Silv.	2.47[−17]	2.28[−17]	2.68[−17]	2.39[−17]	1.74[−17]
200	Hyll.	1.11[−17]	1.04[−17]	1.20[−17]	1.10[−17]	7.21[−18]
	Silv.	9.93[−18]	8.80[−18]	1.11[−17]	9.56[−18]	6.35[−18]
400	Hyll.	9.42[−19]	7.62[−19]	1.09[−18]	8.67[−19]	4.74[−19]
	Silv.	8.64[−19]	6.72[−19]	1.03[−18]	8.00[−19]	4.21[−19]
500	Hyll.	3.95[−19]	2.98[−19]	4.64[−19]	3.47[−19]	1.81[−19]
	Silv.	3.66[−19]	2.69[−19]	4.46[−19]	3.30[−19]	1.61[−19]
750	Hyll.	7.45[−20]	4.81[−20]	8.97[−20]	5.89[−20]	2.85[−20]
	Silv.	7.05[−20]	4.60[−20]	8.84[−20]	5.93[−20]	2.58[−20]
1000	Hyll.	2.14[−20]	1.21[−20]	2.61[−20]	1.54[−20]	7.17[−21]
	Silv.	2.05[−20]	1.21[−20]	2.61[−20]	1.62[−20]	6.57[−21]
1500	Hyll.	3.39[−21]	1.59[−21]	4.19[−21]	2.11[−21]	9.52[−22]
	Silv.	3.30[−21]	1.69[−21]	4.26[−21]	2.35[−21]	8.83[−22]
2000	Hyll.	8.64[−22]	3.55[−22]	1.07[−21]	4.85[−22]	2.17[−22]
	Silv.	8.50[−22]	3.92[−22]	1.10[−21]	5.58[−22]	2.03[−22]
2500	Hyll.	2.90[−22]	1.08[−22]	3.61[−22]	1.50[−22]	6.76[−23]
	Silv.	2.87[−22]	1.23[−22]	3.73[−22]	1.77[−22]	6.37[−23]
3000	Hyll.	1.16[−22]	4.05[−23]	1.45[−22]	5.68[−23]	2.57[−23]
	Silv.	1.15[−22]	4.68[−23]	1.50[−22]	6.81[−23]	2.43[−23]

$$N = \frac{1}{\pi}\left[\frac{1}{\alpha_1^3} + \frac{1}{\alpha_2^3} + \frac{16}{(\alpha_1+\alpha_2)^3}\right]. \tag{34}$$

Here, the following values of the variationally determined parameters and the binding energies are used for (i) $He(1s^2)$; $\alpha_1=2.183\,171$, $\alpha_2=1.188\,53$, and $E_f=-2.875\,661\,4$ and (ii) $Li^+(1s^2)$: $\alpha_1=3.294\,909$, $\alpha_2=2.078\,981$, and $E_f=-7.248\,748$. The obtained theoretical total cross sections for reactions (30) and (31) are additionally multiplied by a factor of 2 in order to include the presence of two electrons in the K shell of the helium target. The explicit computations of the total cross sections are carried out only for capture into the final ground state $1s^2$. The results of the computations of the post and prior total cross sections for He^+-H, He^+-He, and Li^{2+}-He collisions are given in Tables I–III and Figs. 1–3. The columns labeled by the symbols Q_{if}^- and Q_{if}^+ refer to the prior and post cross sections obtained with complete perturbations according to Eqs. (11) and (12). The results which are obtained using the additional approximation: $1/R=1/x_1$ in the prior and post version in the Tables I–III, are denoted by Q_1^- and Q_1^+, respectively. In order to examine the relative role of the relevant term for the dynamic electron correlation $1/r_{12}-1/s_2$ in the prior version, we have also computed the total cross sections by ignoring this term, and the associated results in Tables I–III are denoted by Q_2^-. The total cross sections obtained by means of the Hylleraas wave function [32] for the final heliumlike ground state are labeled as "Hyll" in Tables I–III, while the results denoted by "Silv" are derived utilizing the two-parameter orbitals of Ref. [33].

In Fig. 1 we compare our theoretical results for prior (solid line) and post (dashed line) cross sections for a He^+-H collision, together with a number of experimental data. As can be seen from this figure, the post and prior calculations yield very similar results. The cross sections of the CDW-4B approximation are seen to be in very good agreement with measurements at impact energies $E \geqslant 100$ keV. As can be expected, the CDW-4B model overestimates experimental data at lower impact energies. The results obtained by utilizing the one-parameter wave function [32], as well as the orbital of Silverman *et al.* [33], are close to each other (see the rows denoted by "Hyll" and "Silv" in Table I). Therefore the results related to the Hylleraas wave function are not included in the comparison in Fig. 1.

The results from the CDW-4B method for the He^+-He collisions in the energy range from 50 to 5000 keV/amu are depicted in Fig. 2 and Table II. A comparison between the theoretical results and numerous experimental data shown in this figure reveals overall good agreement. As can be seen, the difference between the two theoretical curves (prior and post) becomes more significant at higher impact energies. At lower energies, the prior and post cross sections are similar,

TABLE III. Same as in Table I except for reaction $^7Li^{2+}+{}^4He \rightarrow {}^7Li^{+}+{}^4He^{+}$.

E (keV)	$\varphi_f(\vec{s}_1,\vec{s}_2)$	Q_{if}^-	Q_{if}^+	Q_1^-	Q_1^+	Q_2^-
1000	Hyll.	4.87[−17]	3.66[−17]	4.75[−17]	3.39[−17]	5.06[−17]
	Silv.	4.75[−17]	3.55[−17]	4.66[−17]	3.29[−17]	4.95[−17]
1500	Hyll.	1.86[−17]	1.39[−17]	1.86[−17]	1.34[−17]	1.78[−17]
	Silv.	1.79[−17]	1.32[−17]	1.79[−17]	1.28[−17]	1.71[−17]
2000	Hyll.	8.43[−18]	6.24[−18]	8.55[−18]	6.14[−18]	7.65[−18]
	Silv.	8.02[−18]	5.83[−18]	8.20[−18]	5.78[−18]	7.25[−18]
3000	Hyll.	2.39[−18]	1.71[−18]	2.47[−18]	1.74[−18]	2.00[−18]
	Silv.	2.25[−18]	1.57[−18]	2.36[−18]	1.61[−18]	1.87[−18]
4000	Hyll.	8.82[−19]	6.10[−19]	9.27[−19]	6.33[−19]	6.94[−19]
	Silv.	8.32[−18]	5.56[−19]	8.86[−19]	5.87[−19]	6.48[−19]
5000	Hyll.	3.85[−19]	2.57[−19]	4.09[−19]	2.71[−19]	2.89[−19]
	Silv.	3.64[−19]	2.35[−19]	3.93[−19]	2.53[−19]	2.70[−19]
7000	Hyll.	1.01[−19]	6.33[−20]	1.09[−19]	6.85[−20]	7.02[−20]
	Silv.	9.67[−20]	5.88[−20]	1.06[−19]	6.52[−20]	6.61[−20]
10000	Hyll.	2.22[−20]	1.27[−20]	2.43[−20]	1.41[−20]	1.41[−20]
	Silv.	2.14[−20]	1.21[−20]	2.39[−20]	1.39[−20]	1.34[−20]
12000	Hyll.	6.83[−21]	5.35[−21]	7.55[−21]	6.03[−21]	4.05[−21]
	Silv.	9.57[−21]	5.20[−21]	1.08[−20]	6.03[−21]	5.71[−21]
14000	Hyll.	4.86[−21]	2.53[−21]	5.38[−21]	2.83[−21]	2.83[−21]
	Silv.	4.75[−21]	2.49[−21]	5.37[−21]	2.93[−21]	2.72[−21]
16000	Hyll.	2.60[−21]	1.30[−21]	2.89[−21]	1.50[−20]	1.46[−21]
	Silv.	2.56[−21]	1.30[−21]	2.91[−21]	1.54[−21]	1.42[−21]
18000	Hyll.	1.48[−21]	7.16[−22]	1.66[−21]	8.33[−22]	8.11[−22]
	Silv.	1.46[−21]	7.26[−22]	1.67[−21]	8.69[−22]	7.87[−22]
20000	Hyll.	8.93[−22]	4.17[−22]	1.00[−21]	4.89[−22]	4.75[−22]
	Silv.	8.84[−22]	4.27[−22]	1.01[−21]	5.15[−22]	4.63[−22]

but they both overestimated the experimentally measured data. On the other hand, the presented CDW-4B model gives better agreement with the experimental findings than in the case of the CB1-4B approximation from Ref. [20].

The theoretical results for the formation of the Li^+ ion in the Li^{2+}-He collisions at energies 1000–20 000 keV are plotted in Fig. 3. Our total cross sections are compared with the experimental data of Woitke *et al.* [6]. A comparison of the prior and post version with measurements [6] shows that the prior variant is slightly superior in reproducing the experimental data. This may be attributed to the fact that the prior form from Eq. (12) contains the term $1/r_{12}$, which explicitly accounts for the dynamical correlations.

The discrepancy between the post and prior cross sections depends essentially on the level of approximation made to determine the ground state wave function of the heliumlike atom. Such a discrepancy is seen in Tables I–III to be much larger in the case of He^+-He and Li^{2+}-He than for He^+-H collisions. For example, at 1000 keV/amu the relative post-prior discrepancy $\delta=|Q_{if}^- - Q_{if}^+|/Q_{if}^-$ is 41%, 39%, and 2% for He^+-He, Li^{2+}-He and He^+-H collisions, respectively, when the Silverman orbital [33] is used for the final bound heliumlike state. The following values for δ are, respectively, obtained: 43%, 41%, and 3% when the Hylleraas function [32] is used for the final states of $He(1s^2)$ and $Li^+(1s^2)$. In the former two cases (He^+-He, Li^{2+}-He), an additional RHF approximation is employed for describing the captured electron. As such, we have obtained a much larger post-prior discrepancy for these two processes than in the case of a He^+-H collision. Of course, the post-prior discrepancy would not exist if all the exact wave functions were available.

The presented four-body treatment allows us to study the contribution of the term $Z_T(1/R-1/x_1)$. The corresponding prior and post cross sections derived by ignoring this term are reported in Tables I–III and labeled by Q_1^- and Q_1^+, respectively. A comparison between the values of Q_{if}^- and Q_1^- shows that the relative contribution of this term does not exceed 20% for He^+-H and Li^{2+}-He collisions and 30% for a He^+-He collision, in the considered energy intervals. This term also has a similar influence on the results obtained in the case of the post formalism. Potential $-Z_T/x_1$ has the asymptotic value $-Z_T/R$ at large distances between Z_T and electron e_1. In such a way, we can estimate the error which is made in a rougher computation which used the additional approximation $1/R=1/x_1$.

The omission of the relevant term for the dynamic electron correlation $1/r_{12}-1/s_2$ from Eq. (12) in the prior version leads to the results presented in Tables I–III via the

columns labeled by Q_2^-. As is shown, the difference between the first column (Q_{if}^-), obtained with the complete perturbation potentials, and the last column (Q_2^-) becomes more significant at higher impact energies. For example, the relative contribution of the correlation term, expressed via $\gamma=|Q_{if}^- - Q_2^-|/Q_{if}^-$ is 62%, 68%, and 32%, respectively, for single capture in He^+-He, Li^{2+}-He, and He^+-H collisions at impact energy 1000 keV/amu, if the final bound heliumlike state is described by Silverman *et al.* [33]. It should be noted that the electron correlation effect is less important for the Li^{2+} projectile due to a higher nuclear charge. Quite similar values of γ via 61%, 67%, and 31% are obtained when the one-parameter Hylleraas orbital [32] is used for the final state of (Z_P,e_1,e_2). This means that the dynamic electron correlations play a very important role, especially at higher impact energies. A similar conclusion has been previously reached in Refs. [21–23] for single electron capture in collisions between completely stripped projectiles and heliumlike targets.

IV. CONCLUSIONS

We have studied single charge exchange in collisions of hydrogenlike projectiles with atomic hydrogen as well as multielectron atoms by employing the CDW-4B approximation at intermediate and high impact energies. The CDW-4B method is used for computing the post and prior total cross sections in He^+-H, He^+-He, and Li^{2+}-He collisions. The relative importance of the various terms in the complete perturbation potential is thoroughly investigated. The prior version of the CDW-4B approximation explicitly includes the dynamic electron correlations through the dielectronic interactions in the transition amplitude. The presented theoretical results for total cross sections indicate that dynamic electron correlations are important, especially at higher impact energies for the considered processes. The agreement between the cross sections obtained via the CDW-4B and the corresponding experimental data is very good at intermediate and high energies.

ACKNOWLEDGMENTS

Thanks are due to Professor Dž. Belkić for helpful discussions and a critical review of the paper. The author gratefully acknowledges the financial support from Ministry of Science of the Republic of Serbia through Project No. 141029A.

[1] H. Atan, W. Steckelmacher, and M. W. Lucas, J. Phys. B **24**, 2559 (1991).
[2] J. L. Forest, J. A. Tanis, S. M. Ferguson, R. R. Haar, K. Lifrieri, and V. L. Plano, Phys. Rev. A **52**, 350 (1995).
[3] R. D. DuBois, Phys. Rev. A **39**, 4440 (1989).
[4] P. Hvelplund and A. Andersen, Phys. Scr. **26**, 375 (1982).
[5] N. V. de Castro Faria, F. L. Freire, Jr., and A. G. de Pinho, Phys. Rev. A **37**, 280 (1988).
[6] O. Woitke, P. A. Závodszky, S. M. Ferguson, J. H. Houck, and J. A. Tanis, Phys. Rev. A **57**, 2692 (1998).
[7] R. E. Olson, A. Salop, R. A. Phaneuf, and F. W. Mayer, Phys. Rev. A **16**, 1867 (1977).
[8] M. B. Shah, T. V. Goffe, and H. B. Gilbody, J. Phys. B **11**, L233 (1978).
[9] J. G. Murphy, K. F. Dunn, and H. B. Gilbody, J. Phys. B **27**, 3687 (1994).
[10] A. Itoh, M. Asari, and F. Fukuzawa, J. Phys. Soc. Jpn. **48**, 943 (1980).
[11] L. I. Pivovar, V. M. Tabuev, and M. T. Novikov, Zh. Eksp. Teor. Fiz. **41**, 26 (1961) [Sov. Phys. JETP **14**, 20 (1962)].
[12] M. Purkait, Nucl. Instrum. Methods Phys. Res. B **207**, 101 (2003).
[13] A. Dhara, M. Purkait, S. Sounda, and C. R. Mandal, Indian J. Phys. **75B**, 85 (2001).
[14] J. K. M. Eichler, A. Tsuji, and T. Ishihara, Phys. Rev. A **23**, 2833 (1981).
[15] Dž. Belkić, Phys. Scr. **43**, 561 (1991).
[16] R. L. Becker and A. D. MacKellar, J. Phys. B **12**, L345 (1979).
[17] R. E. Olson and A. Salop, Phys. Rev. A **16**, 531 (1977).
[18] M. Das, M. Purkait, and C. R. Mandal, Eur. Phys. J. D **8**, 13 (2000).
[19] I. Mančev, Phys. Scr. **51**, 762 (1995).
[20] I. Mančev, Phys. Rev. A **54**, 423 (1996).
[21] Dž. Belkić, R. Gayet, J. Hanssen, I. Mančev, and A. Nunez, Phys. Rev. A **56**, 3675 (1997).
[22] I. Mančev, Phys. Rev. A **60**, 351 (1999).
[23] Dž. Belkić, J. Comput. Methods Sci. Eng. **1**, 1 (2001).
[24] Dž. Belkić, J. Phys. B **30**, 1731 (1997).
[25] Dž. Belkić, *Principles of Quantum Scattering Theory* (The Institute of Physics Publishing, Bristol, England, 2004), and references therein.
[26] Dž. Belkić, I. Mančev, and J. Hanssen, Rev. Mod. Phys. (to be published 2007).
[27] R. T. Pedlow, S. F. C. O'Rourke, and D. S. F. Crothers, Phys. Rev. A **72**, 062719 (2005).
[28] D. S. F. Crothers and L. Dubé, Adv. At., Mol., Opt. Phys. **30**, 287 (1993).
[29] Dž. Belkić, R. Gayet, and A. Salin, Phys. Rep. **56**, 279 (1979).
[30] E. Clementi and C. Roetti, At. Data Nucl. Data Tables **14**, 177 (1974).
[31] A. Nordsieck, Phys. Rev. **93**, 785 (1954).
[32] E. Hylleraas, Z. Phys. **54**, 347 (1929).
[33] J. N. Silverman, O. Platas, and F. A. Matsen, J. Chem. Phys. **32**, 1402 (1960); C. Eckart, Phys. Rev. **36**, 878 (1930).
[34] M. B. Shah and H. B. Gilbody (private communication).